Biomedicine & Pharmacotherapy 177 (2024) 117076

Contents lists available at ScienceDirect

Biomedicine & Pharmacotherapy

journal homepage: www.elsevier.com/locate/biopha

Inhibitors of the tyrosine kinases FMS-like tyrosine kinase-3 and WEE1 induce apoptosis and DNA damage synergistically in acute myeloid leukemia cells

Christoph Hieber [a,b,1], Al-Hassan M. Mustafa [a,c,1], Sarah Neuroth [a], Sven Henninger [a], Hans-Peter Wollscheid [d], Joanna Zabkiewicz [e], Michelle Lazenby [e], Caroline Alvares [e], Siavosh Mahboobi [f], Falk Butter [d,g], Walburgis Brenner [h], Matthias Bros [b,2], Oliver H. Krämer [a,*,2]

[a] Institute of Toxicology, University Medical Center of Johannes Gutenberg University Mainz, Mainz 55131, Germany
[b] Department of Dermatology, University Medical Center of Johannes Gutenberg University Mainz, Mainz 55131, Germany
[c] Department of Zoology, Faculty of Science, Aswan University, Aswan, Egypt
[d] Institute of Molecular Biology, Ackermannweg 4, Mainz 55128, Germany
[e] Department of Haematology, Cardiff Experimental Cancer Medicine Centre, Cardiff University, Wales, UK
[f] Institute of Pharmacy, Faculty of Chemistry and Pharmacy, University of Regensburg, Regensburg 93040, Germany
[g] Institute of Molecular Virology and Cell Biology (IMVZ), Friedrich Loeffler Institute, Greifswald 17493, Germany
[h] Department of Obstetrics and Gynecology, University Medical Center, Mainz 55131, Germany

ARTICLE INFO

Keywords:
AML
DNA replication stress
FLT3-ITD
Inhibitors
Synergism
WEE1

ABSTRACT

Hyperactive FMS-like receptor tyrosine kinase-3 mutants with internal tandem duplications (FLT3-ITD) are frequent driver mutations of aggressive acute myeloid leukemia (AML). Inhibitors of FLT3 produce promising results in rationally designed cotreatment schemes. Since FLT3-ITD modulates DNA replication and DNA repair, valid anti-leukemia strategies could rely on a combined inhibition of FLT3-ITD and regulators of cell cycle progression and DNA integrity. These include the WEE1 kinase which controls cell cycle progression, nucleotide synthesis, and DNA replication origin firing. We investigated how pharmacological inhibition of FLT3 and WEE1 affected the survival and genomic integrity of AML cell lines and primary AML cells. We reveal that promising clinical grade and preclinical inhibitors of FLT3 and WEE1 synergistically trigger apoptosis in leukemic cells that express FLT3-ITD. An accumulation of single and double strand DNA damage precedes this process. Mass spectrometry-based proteomic analyses show that FLT3-ITD and WEE1 sustain the expression of the ribonucleotide reductase subunit RRM2, which provides dNTPs for DNA replication. Unlike their strong pro-apoptotic effects on leukemia cells with FLT3-ITD, inhibitors of FLT3 and WEE1 do not damage healthy human blood cells and murine hematopoietic stem cells. Thus, pharmacological inhibition of FLT3-ITD and WEE1 might become an improved, rationally designed therapeutic option.

1. Introduction

The FMS-like tyrosine kinase-3 (FLT3) ligand activates the FLT3 receptor tyrosine kinase transiently during hematopoiesis. Over 23 % of acute myeloid leukemia (AML) patients carry mutations in the tyrosine kinase FLT3. These give rise to constitutively active FLT3 mutant molecules that promote cell proliferation and the resistance of leukemic cells to apoptosis (programmed cell death). Common FLT3 mutations

* Corresponding author.
E-mail addresses: chieber@uni-mainz.de (C. Hieber), alabdeen@uni-mainz.de (A.-H.M. Mustafa), neuroths@uni-mainz.de (S. Neuroth), svjhenninger@gmail.com (S. Henninger), hwollsch@uni-mainz.de (H.-P. Wollscheid), ZabkiewiczJ1@cardiff.ac.uk (J. Zabkiewicz), LazenbyM@cardiff.ac.uk (M. Lazenby), AlvaresC@cardiff.ac.uk (C. Alvares), Siavosh.mahboobi@chemie.uni-regensburg.de (S. Mahboobi), F.Butter@imb-mainz.de, f.butter@imb.de (F. Butter), brenner@uni-mainz.de (W. Brenner), mbros@uni-mainz.de (M. Bros), okraemer@uni-mainz.de (O.H. Krämer).
[1] equal first author contribution
[2] equal last author contribution

https://doi.org/10.1016/j.biopha.2024.117076
Received 21 April 2024; Received in revised form 16 June 2024; Accepted 29 June 2024
Available online 5 July 2024
0753-3322/© 2024 The Author(s). Published by Elsevier Masson SAS. This is an open access article under the CC BY license (http://creativecommons.org/licenses/by/4.0/).

are internal tandem duplications in the juxtamembrane domain or in the first part of its kinase domain (FLT3-ITD) and point mutations in the second FLT3 tyrosine kinase domain (TKD) of FLT3 [1–4].

The poor prognosis of AML patients with FLT3-ITD has spurred an intensive search for tyrosine kinase inhibitors (TKi) against FLT3. Quizartinib is a highly specific FLT3 inhibitor that produces promising benefits in FLT3-ITD-positive AML patients [5]. Incomplete hematopoietic recovery and secondary resistance mutations in the FLT3-TKD arise during therapy with quizartinib. These findings verify that FLT3-ITD is a driver of the disease and not just a bystander mutation [6]. In Japan, quizartinib is approved for the treatment of adults with relapsed/refractory FLT3-ITD-positive AML cells. In a worldwide phase III clinical study, quizartinib increased the overall survival of 294 male and 245 female patients from 18 to 75 years with newly diagnosed FLT3-ITD-positive AML cells. This benefit was achieved upon combination of quizartinib with the DNA-damaging drugs cytarabine and daunorubicin/idarubicin and occurred at low side effects [5]. Currently, the TKi midostaurin and gilteritinib are in worldwide clinical use for patients with FLT3-mutated AML [3,4]. Disadvantages of these drugs are their broad inhibitory profiles against various kinases and associated side-effects, including a possible breakdown of normal hematopoiesis [7–9]. Furthermore, the mutation N676K in the FLT3-TKD confers resistance to midostaurin [10,11]. We have recently identified and patented the inhibitor marbotinib, which targets the allosteric back pocket and the ATP binding pocket of FLT3. These structural features allow marbotinib and its water-soluble derivative marbotinib-carbamate to act as highly specific, nanomolar inhibitors of FLT3-ITD and FLT3-TKD in cells and in vivo [9,12]. It is currently unknown if anti-leukemic effects of marbotinib can be augmented in combination schemes.

AML, acute lymphoid leukemia (ALL), multiple myeloma, chronic myeloid and lymphoid leukemia, and diffuse large B cell lymphoma samples [13] frequently overexpress the tyrosine kinase WEE1. This enzyme prevents premature traversal of cells into G2/M phase when DNA is incompletely repaired or damaged [13–15]. WEE1 phosphorylates and consequently inhibits the cyclin-dependent kinases CDK1/CDK2, which promote DNA origin firing for cell cycle entry and cell cycle progression [13,14,16]. It is also known that WEE1 suppresses CDK1/CDK2 to prevent the degradation of nascent DNA at stalled replication forks by the nucleolytic enzymes DNA2 [17] and MUS81 [18–20] in solid tumor-derived cells. Moreover, WEE1 ensures histone gene transcription during S phase in such cells [21]. In long-term cultured and freshly isolated AML and ALL cells, WEE1 promotes the major DNA repair pathway of homologous recombination (HR) and thereby suppresses DNA damage [22]. Furthermore, WEE1 ensures the supply of deoxyribonucleotides (dNTPs) for DNA replication. In this regard, WEE1 induces the transcription and decreases the protein turnover of the ribonucleotide reductase subunit RRM2, which is inevitable for dNTP synthesis [18,23,24]. Although it is known that solid tumor-derived cells with reduced or inhibited RRM2 are hypersensitive to WEE1 inhibitors [23], it is still unknown if this applies to leukemic cells and if this is therapeutically relevant.

In addition to WEE1, the serine/threonine kinase checkpoint kinase-1 (CHK1) restricts the activities of CDK1/CDK2. CHK1 inhibits the CDK-activating CDC25 phosphatases by phosphorylation and thereby promotes the inhibitory phosphorylation of these CDKs [25]. Pharmacological inhibition of both WEE1 and CHK1 compromises genomic integrity and the survival of cancer cells [14,26]. Curiously, the expression of hyperactive FLT3 promotes the expression of CHK1 by epigenetic mechanisms but attenuates the expression of WEE1 in leukemia cell cultures and primary AML cells [27,28]. Nonetheless and partially contrasting these findings, FLT3 inhibitors decrease both CHK1 and WEE1 in AML cells with FLT3-ITD [29]. The WEE1 inhibitor adavosertib (MK1775) is the best-established inhibitor of this kinase and currently used in clinical trials that involve leukemia patients [30–34]. This drug may be useful for the treatment of patients with mutant FLT3, in which WEE1 promotes resistance of AML cells with FLT3-TKD towards midostaurin [35]. Despite these insights, the molecular mechanisms through which inhibitors of FLT3 and WEE1 kill leukemic cells carrying FLT3 mutants are ill-defined.

According to current knowledge, FLT3 inhibitors develop their full clinical potential in rationally designed combination therapies [2–4]. Here we show that inhibitors of FLT3 and WEE1 synergistically induce apoptosis of leukemic cells with mutant FLT3. This is associated with DNA replication stress, DNA damage, and a loss of the vital enzyme RRM2 that supplies dNTPs.

2. Results

2.1. Inhibitors of FLT3 and WEE1 induce apoptosis synergistically in AML cells with FLT3-ITD

MV4–11 cells were established from a 10-year-old boy with acute monocytic leukemia (AML FAB M5). They carry two copies of FLT3-ITD and the AF4-MLL1 translocation t (4;11). These are intermediate to unfavorable prognostic markers. We evaluated if well-characterized FLT3 and WEE1 inhibitors kill such cells. We treated MV4–11 cells with quizartinib, adavosertib, and combinations thereof for 24 h. Based on literature data [9,12,21,22], we used 1–5 nM quizartinib and 200–500 nM adavosertib (30 drug combinations in total). We assessed mitochondrial depolarization as an early apoptosis marker using the mitochondrial integrity dye 3,3′-dihexyloxacarbocyaniniodid (DIOC6) and the accumulation of the DNA-binding dye 4′,6-diamidin-2-phenylindol (DAPI) as a late apoptosis marker of cells with impaired efflux capacity. Quizartinib and adavosertib induced the accumulation of early and late apoptotic cells dose-dependently. Combinations of these drugs induced apoptosis more effectively than the single agents (Fig. 1A).

We evaluated whether the effects of these combinations are synergistic with the combenefit program, which uses the algorithms Loewe, Bliss, and HSA [36]. All 30 drug concentrations induced apoptosis synergistically and significantly in MV4–11 cells (Fig. 1B).

We complemented these data with cell cycle analyses, including the detection of subG1 fractions as late apoptosis marker (cell fragments with DNA contents below 2 n). Quizartinib dose-dependently reduced the numbers of cells in the S and G2/M phases of the cell cycle. Adavosertib dose-dependently decreased all vital cell cycle phases about equally. These alterations were associated with a dose-dependent accumulation of the subG1 phase. Combined application of quizartinib plus adavosertib depleted cells in both S and G2/M phases more strongly than the single drug applications did (supplementary Fig. S1A). The accumulation of MV4–11 cells in subG1 phase was increased synergistically and significantly upon treatment with 13 drug combinations (supplementary Fig. S1B).

To extend these findings using a translational setting, we treated primary human AML cells carrying wild-type FLT3 or FLT3-ITD with quizartinib and adavosertib at doses ranging from 0 to 5 μM. Nanomolar concentrations of quizartinib sufficed to reduce the proliferation of FLT3-ITD-positive AML cells but not of AML cells with wild-type FLT3. Adavosertib was comparably effective against AML cells, irrespective of FLT3 mutations. Quizartinib plus adavosertib synergistically eliminated FLT3-ITD-positive AML cells and overcame a plateau of drug efficacy that occurred when using the single drugs. Curiously, low doses of quizartinib that did not affect the FLT3 wild-type AML cells exerted an inhibitory effect in combination with adavosertib against such cells (Fig. 1C).

Prompted by this finding, we conducted a CRISPR-Cas9 knockout data search using The Cancer Dependency Map Project at Broad Institute (DepMap). We analyzed the reliance of 37 AML cell types on FLT3 and WEE1. AML cells with mutant FLT3 were most dependent on FLT3 (MOLM-13, MV4–11, MOLM-14, Monomac-6) but the proliferation of one FLT3 wild-type AML cell line (NOMO1 [37]) was also reduced by a

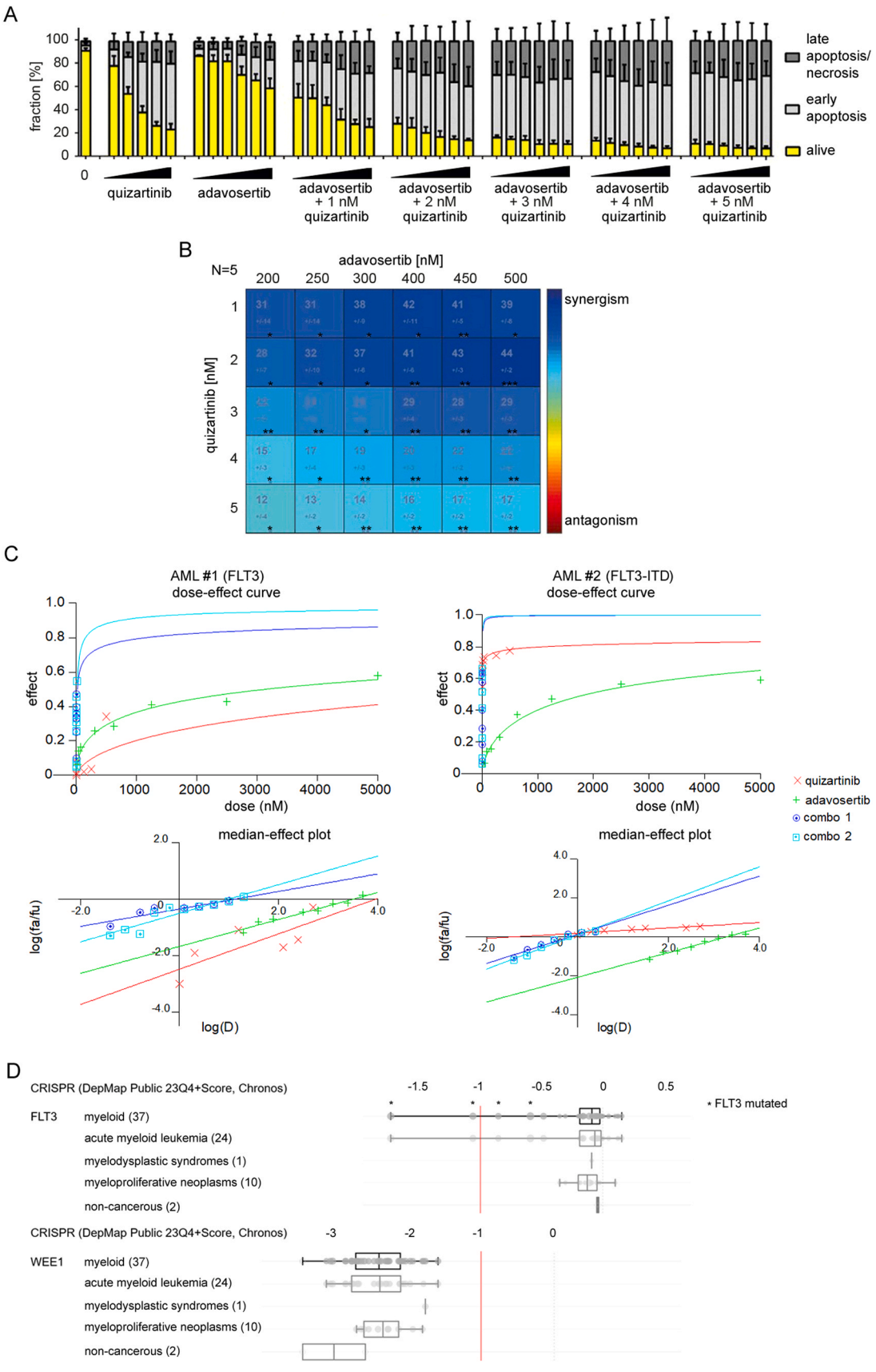

(caption on next page)

Fig. 1. Synergistic cell death induction upon inhibition of FLT3 and WEE1. **A**: MV4–11 cells were treated for 24 h with 1/2/3/4/5 nM quizartinib and 200/250/300/400/450/500 nM adavosertib; 0, solvent-treated control cells. Cells were harvested and stained with DIOC6 and DAPI. DIOC6-positive cells are alive, with intact mitochondria. DIOC6-negative/DAPI-negative cells are early apoptotic, with a decrease of DIOC6 due mitochondrial injury. DIOC6-negative/DAPI-positive cells are late apoptotic, with disrupted mitochondria and disrupted plasma membrane integrity. Shown are average values from 4 independent experiments. **B**: The combenefit program uses the algorithms Loewe, Bliss, and HSA to unravel synergism. Shown are synergism scores and significances (n=4±SD, *p<0.05; **p<0.01; ***p<0.001). **C**: Primary human AML cells with FLT3-ITD are susceptible to quizartinib and adavosertib. Dose-effect curves show synergistic responses of primary AML blasts to quizartinib and adavosertib after 72 h (range: 0–5000 nM; combo 1 quizartinib:adavosertib=1:1000, combo 2 quizartinib:adavosertib=1:500). AML#1 (FLT3/NPM1 mutant, age 73, favorable cytogenetics), AML#2 (FLT3-ITD/NPM1 mutant, age 74, intermediate cytogenetic risk); effect: 0 = proliferation unaffected and 1 = 100 % growth inhibition. **D**: DepMap project data show the dependency of myeloid leukemia cells on FLT3 and WEE1; the dependency cutoff is −1 and indicated by a red line. Essential genes have a dependency score of −1 and less (up to 100 % counterselection against cells with the knockdown, growth arrest or killing; https://forum.depmap.org/t/depmap-genetic-dependencies-faq/131).

knockout of FLT3. Independent of their FLT3 status, all AML cell types were highly reliant on WEE1 (Fig. 1D). Such data are coherent with data shown in Fig. 1A-C.

These results demonstrate that concurrent inhibition of FLT3 and WEE1 is synergistically lethal for leukemic cells with hyperactive FLT3.

2.2. Inhibitors of FLT3 and WEE1 combine their on-target activities

These data encouraged us to scrutinize the impact of quizartinib and adavosertib on signaling through FLT3-ITD and WEE1. Quizartinib suppressed the phosphorylation of FLT3-ITD. This led to an accumulation of the slower migrating, hyperglycosylated, mature form of FLT3-ITD. Accordingly, quizartinib impaired the phosphorylation of the FLT3-ITD target proteins ERK1/ERK2, STAT5, AKT, and p38. Adavosertib dose-dependently stabilized FLT3-ITD modestly. Quizartinib plus adavosertib eliminated total and phosphorylated FLT3-ITD. Adavosertib did not affect ERK and p38 expression but slightly reduced the levels of AKT and STAT5 at 400–450 nM. Quizartinib plus adavosertib decreased phosphorylated and total STAT5, AKT, and p38 (Fig. 2A).

We evaluated the on-target activity of adavosertib by measuring the phosphorylation of the WEE1 target CDK1 by immunoblot. Adavosertib blocked the phosphorylation of CDK1 rapidly. This was also the case for the adavosertib plus quizartinib combination. Coherent with the time-delayed inhibition of WEE1 expression by quizartinib [29], it produced a delayed loss of CDK1 phosphorylation (Fig. 2B). Adavosertib has a very mild impact on total WEE1, which confirms that this agent is a direct, reversible inhibitor of the catalytic activity of WEE1 (supplementary Fig. S2A).

Since CHK1 promotes resistance against adavosertib in leukemic cells [38], we analyzed its levels. Adavosertib and quizartinib reduced CHK1 levels alone and in combination (Fig. 2B).

These data demonstrate that quizartinib and adavosertib combinations sum up in their effects on cell signaling cascades. This corresponds to their joined negative impact on AML cell survival.

2.3. Dysregulation of apoptosis regulators by inhibitors of FLT3 and WEE1

Quizartinib and adavosertib disrupt mitochondrial integrity (Fig. 1A, B), which is controlled by pro-apoptotic and anti-apoptotic proteins of the BCL2 family [39,40]. Therefore, we examined the levels of such proteins in MV4–11 cells treated with quizartinib and adavosertib. The pro-apoptotic proteins BAK and BAX form pores that allow the leakage of cytochrome c from mitochondria and the subsequent activation of caspases that propel apoptosis [39]. BAK was expressed in MV4–11 cells and the drugs did not alter its levels (Fig. 3A). The pro-apoptotic BH3-only BCL2 family member BIM activates BAK/BAX complexes [39]. Quizartinib alone and quizartinib plus adavosertib caused an accumulation of BIM (Fig. 3A).

MCL1 exerts anti-apoptotic functions as full-length protein but its smaller isoform augments the sensitivity of cells to pro-apoptotic stimuli [39,40]. Quizartinib and adavosertib attenuated full-length MCL1 dose-dependently (Fig. 3A). When we analyzed another anti-apoptotic protein, BCL2, we noted that these drugs marginally reduced its levels

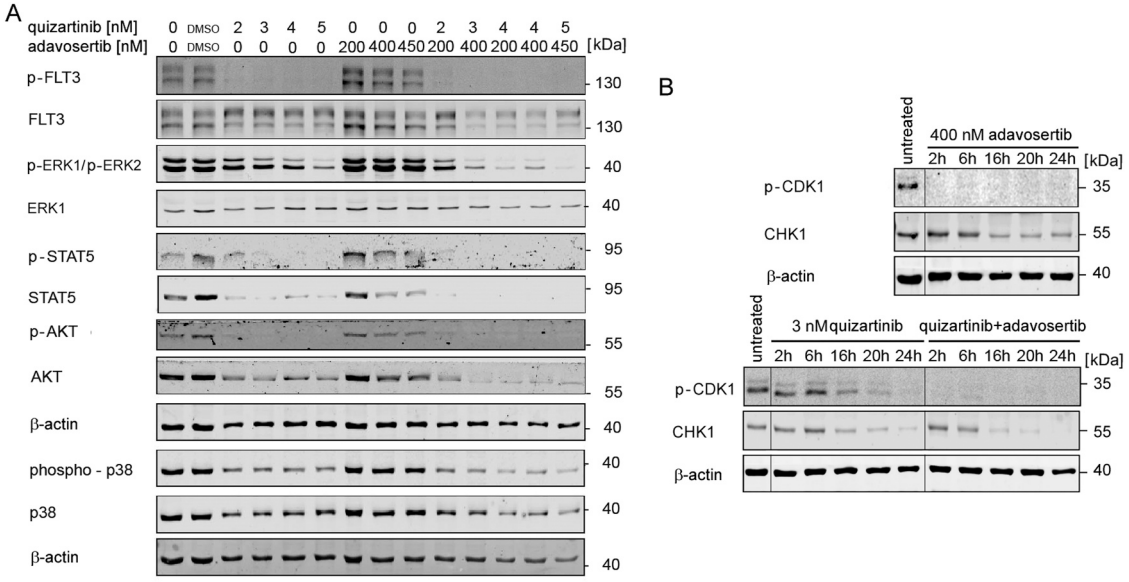

Fig. 2. Simultaneous inhibition of FLT3 and WEE1 downstream signaling. A: Phosphorylation and expression of FLT3-ITD and its targets ERK1/ERK2, STAT5, AKT, and p38 were analyzed by immunoblot of lysates from MV4–11 cells. These were incubated with quizartinib and adavosertib as indicated for 24 h; 0, untreated control; DMSO, solvent control; β-actin as loading control (n=3). B: MV4–11 cells were treated as indicated for 2–24 h. Immunoblot analyses revealed the phosphorylation of the WEE1 target protein CDK1 and CHK1 protein levels; β-actin as loading control; (n=3).

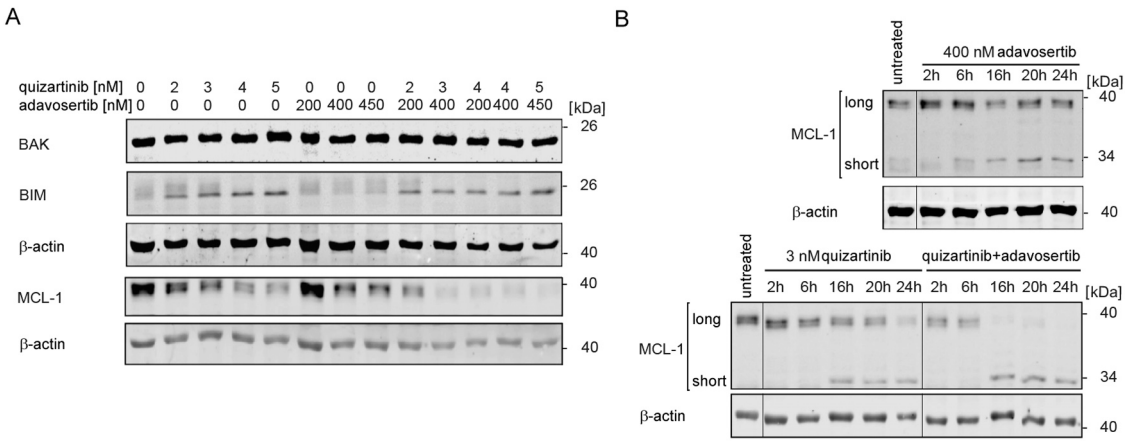

Fig. 3. Simultaneous inhibition of FLT3 and WEE1 modulates apoptosis regulators. A: Immunoblot analysis of pro- and anti-apoptotic proteins after the indicated treatments with quizartinib and adavosertib for 24 h; β-actin serves as loading control on independent membranes; (n=3). B: Immunoblot analyses of MCL1 in MV4–11 cells that were treated with the indicated concentrations of adavosertib (400 nM) and quizartinib (3 nM). β-actin serves as loading control (n=3).

in MV4–11 cells (supplementary Fig. S2A). This was also the case in human FLT3-ITD/FLT3-positive MOLM-13 cells (supplementary Fig. S2B), which are from the peripheral blood of a 20-year-old man with AML after myelodysplastic syndrome.

To study the regulation of MCL1 by the chosen drug regimen further, we conducted time course experiments with a synergistically pro-apoptotic combination of quizartinib and adavosertib. We chose 3 nM quizartinib plus 400 nM adavosertib, because flow cytometry-based assays showed that this combination produced significant, synergistic pro-apoptotic effects in MV4–11 cell cultures (Fig. 1 and supplementary Fig. S1). We analyzed lysates of MV4–11 cells for full-length and short versions of MCL1. Compared to the single drugs, the combination of quizartinib and adavosertib depleted the long MCL1 isoform more rapidly and caused an accumulation of the short MCL1 isoform (Fig. 3B).

The expression, posttranslational modifications, and mutations of the tumor suppressive transcription factor p53 can determine the responsiveness of AML cells to therapies and hence the prognosis of AML patients [41–43]. We assessed the impact of quizartinib and adavosertib on p53, the levels of its prototypical target p21, and activating post-translational modifications of p53 in MV4–11 cells. Quizartinib reduced the phosphorylation of p53, the levels of p53, and p21 expression. Adavosertib augmented p53, its phosphorylation and acetylation, but not p21 expression. In the combination scheme, the negative impact of quizartinib on p53-p21 was stronger than upon treatment with quizartinib alone (supplementary Fig. S3).

These results illustrate that quizartinib and adavosertib modulate key regulators of mitochondrial outer membrane permeabilization and subsequently apoptosis of leukemia cells with FLT3-ITD.

2.4. *Induction of DNA replication stress and DNA damage upon inhibition of FLT3 and WEE1*

Quizartinib and adavosertib stall DNA replication and compromise the integrity of DNA replication forks [9,13,14,16,29]. We used confocal immunofluorescence to specify how combinations of these drugs caused DNA replication stress and DNA damage. We measured single strand DNA stretches as nuclear RPA foci, their conversion into single strand and double strand DNA breaks as nuclear foci containing histone H2A phosphorylated at serine-139 (γH2AX), and DNA double strand breaks as nuclear 53BP1 foci [44–46]. We incubated MV4–11 cells with quizartinib and adavosertib for 6 h. We chose this short incubation period to avoid the detection of DNA damage as a secondary result of apoptosis [45]. Moreover, this experimental setup allowed us to assess if DNA replication stress/DNA damage may precede apoptosis induction by inhibitors of FLT3-ITD and WEE1. Compared to the single treatments, the combination of quizartinib and adavosertib induced significantly higher accumulation of 53BP1, γH2AX, and RPA foci after 6 h (Fig. 4A, B).

Caspase-3 is a definite inducer of apoptosis ("point-of-no-return") that is activated by limited proteolysis [39]. We verified lack of apoptosis induction as absence of caspase-3 cleavage after 6 h (Fig. 4**C**). We congruently noted no increase in annexin-V/PI-positive cells (Supplemental Fig. S4). These findings rule out early and late apoptosis as causes of the DNA replication stress/DNA damage phenotype that we show above.

Since marbotinib is effective against FLT3-ITD with secondary, therapy-associated FLT3-TKD mutants [9,12], we additionally assessed the impact of marbotinib plus adavosertib on murine leukemic Ba/F3 cells that are driven by FLT3-ITD/D835Y. Moreover, we used Ba/F3 FLT3 wild-type cells that grow depending on the cytokine interleukin-3 (IL3). These do not show the typical cancer cell feature of growth factor-independent proliferation and are more related to normal cells in this regard. Adavosertib induced an accumulation of γH2AX in IL3-dependent Ba/F3 cells with wild-type FLT3, but this was not caused by marbotinib. Compared to these cells, IL3-independent Ba/F3 cells with FLT3-ITD/D835Y were less susceptible to adavosertib but sensitive to marbotinib. Remarkably, adavosertib plus marbotinib induced more γH2AX than the single drug treatments in Ba/F3 cells carrying FLT3-ITD/D835Y than in cognate IL3-dependent cells (supplementary Fig. S5). These data support previously reported results [35].

The filament protein RAD51 initiates the repair of broken DNA replication forks through HR. This can suppress cytotoxic effects of DNA-damaging agents [47]. We previously showed that inhibitors of FLT3 reduced the expression of RAD51 [29] and speculated that this correlated with the higher levels of pro-apoptotic DNA lesions in MV4–11 cells that were exposed to FLT3 inhibitors and adavosertib. Immunoblotting of RAD51 with lysates from MV4–11 cells that were incubated with synergistically pro-apoptotic combinations of quizartinib and adavosertib (Fig. 1A,B) revealed that this synergism was linked to decreased levels of RAD51 (Fig. 4D).

To exclude that the impact of drugs blocking FLT3 and WEE1 on DNA integrity results in general toxicity, we incubated human peripheral blood mononuclear cells (PBMCs) with quizartinib and adavosertib. Evaluation of cell vitality as metabolic activity and flow cytometry using live/dead staining showed that both drugs significantly decreased the viability of MV4–11 cells but not of PBMCs (Fig. 4E,F).

The investigation of individual cell populations, including B-cells, T-cells, natural killer (NK) cells, dendritic cells (DCs), and monocytes verified that adavosertib ± quizartinib were not toxic to such primary human blood cells (Fig. 4G).

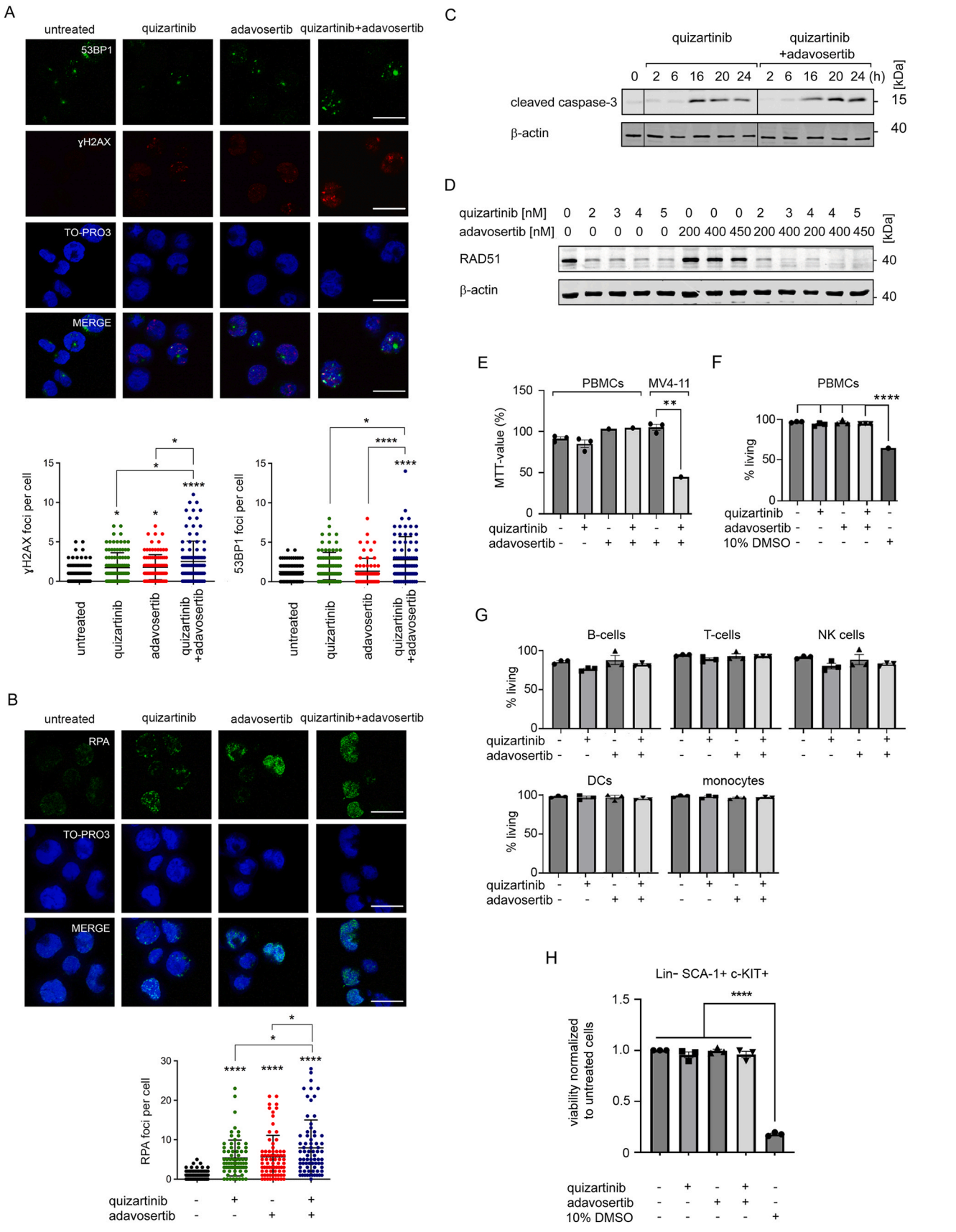

(caption on next page)

Fig. 4. Analysis of DNA lesions that are induced by inhibitors of FLT3 and WEE1. A,B: MV4–11 cells were treated with 3 nM quizartinib ± 400 nM adavosertib for 6 h. Foci of 53BP1 and γH2AX in the nucleus were detected by immunofluorescence, counted (80–100 cells/sample, n=2), and statistically evaluated, one-way ANOVA with Bonferroni multi-comparison test; *p<0.05, ****p<0.001; scale bar, 10 μm. B: MV4–11 cells were treated with 3 nM quizartinib ± 400 nM adavosertib for 6 h. Nuclear RPA foci were detected by immunofluorescence, counted (80–100 cells/sample, n=2), and statistically evaluated, one-way ANOVA with Bonferroni multi-comparison test; *p<0.05, ****p<0.0001; scale bar, 10 μm. C: MV4–11 cells were treated with 3 nM quizartinib ± 400 nM adavosertib for the indicated times. Cells were harvested and analyzed for cleaved caspase-3; β-actin, loading control (n=3). D: RAD51 expression was analyzed by immunoblot of lysates from MV4–11 cells. These were incubated with quizartinib and adavosertib as indicated for 24 h; 0, untreated; β-actin serves as loading control (n=2). E: PBMCs or MV4–11 cells were treated with 3 nM quizartinib ± 400 nM adavosertib for 72 h and analyzed by MTT-test. PBMCs were isolated from blood samples from 3 healthy donors. MV4–11 cells were used as positive control for a drug-induced impact on cell viability. F: The same PBMCs as mentioned in E were analyzed by flow cytometry using the sensitive viability dye eFluor-780. G: analysis of individual cell populations within the analyzed PBMCs by flow cytometry, with antibodies for lineage markers. The groups are B-lymphocytes ($CD3^-CD19^+$), T-lymphocytes ($CD3^+$), NK cells ($CD3^-CD19^-CD56^+$), DCs ($CD3^-CD19^-CD1c^+$), and monocytes ($CD3^-CD19^-CD14^+$). Cell viability was evaluated with annexin-V and FVD staining. H: freshly isolated murine bone marrow cells were treated with 3 nM quizartinib ± 400 nM adavosertib for 24 h. Application of 10 % DMSO served as a positive control for cell death induction. Cells were harvested and analyzed by flow cytometry. The viability of cells that were negative for lineage markers (Lin-; CD3, CD19, CD11b, NK1.1, Gr-1, CD4, CD8) but double-positive for SCA-1 and c-KIT was assessed with the Fixable Viability Dye eFluor® 780. Data denote the mean±SEM of three independent experiments. Single data points are shown. Significant differences were assessed by one-way ANOVA and post-hoc Tukey test (****p<0.0001).

To evaluate the impact of these drugs on primary bone marrow cells, we isolated such cells from bone marrow tissues from the hind legs of C57BL/6 mice and treated cells from each mouse with adavosertib ± quizartinib ex vivo (bone marrow cells treated with a cytotoxic concentration of DMSO served as a controls for cell killing). We analyzed lineage-negative SCA-1/c-KIT-double positive cells representing hematopoietic stem cells (equating to human CD34-positive hematopoietic stem cells) for their viability. In this setting, neither quizartinib, nor adavosertib or their combination decreased the viability of primary hematopoietic stem cells (Fig. 4H).

These data show that the induction of DNA replication stress/DNA damage are early events of apoptosis induction by inhibitors of FLT3 and WEE1 in AML cells with FLT3-ITD, but not in primary differentiated and primitive hematopoietic cells.

2.5. Mechanisms for how inhibitors of FLT3 and WEE1 cause lethal DNA stress

To obtain unbiased, global insights into proteins that are controlled by FLT3-ITD and WEE1, we used mass spectrometry-based proteomics. We treated MV4–11 cells with marbotinib and adavosertib and detected up to 4602 proteins. We chose marbotinib for these tests because it is not vulnerable to the FLT3-TKD escape mutations that arise in quizartinib-treated patients [9,12]. We noted that marbotinib reduced RRM2 and increased FLT3 (Fig. 5A), indicating an accumulation of inhibited FLT3-ITD. Adavosertib augmented the levels of RAD51 (Fig. 5B). Marbotinib plus adavosertib caused a stronger reduction of RRM2 than quizartinib. Unlike the single agents, marbotinib plus adavosertib did not augment FLT3 and RAD51 levels (Fig. 5C). These findings correspond to the immunoblot data for RAD51 (Fig. 4D).

To confirm that marbotinib plus adavosertib is more pro-apoptotic than each agent alone, we probed lysates for activated caspase-3 by immunoblot. We tested this in MOLM-13 and MV4–11 cells. Coherent with the data showing a drug synergism for quizartinib and adavosertib in MV4–11 cells (Fig. 1A,B), caspase-3 activation occurred more pronouncedly in response to the combinatorial treatment than upon the single drug treatments in both cell cultures (Fig. 5D).

According to our proteomic screen, marbotinib alone and combined with adavosertib strongly reduce RRM2 (Fig. 5A-C). To further define the association between RRM2 and the rapid induction of DNA replication stress/DNA damage by quizartinib plus adavosertib, we conducted time course analyses spanning 4, 8, and 16 h. In MOLM-13 cells, 3 nM quizartinib and 400 nM adavosertib decreased RRM2 within early hours after treatment. Inhibition of FLT3-ITD and WEE1 tied in with depletion of WEE1, impaired activation of the FLT3-ITD downstream target proteins STAT5, and stable levels of p38 in MOLM-13 cells (Fig. 5E, left panel). To delineate the contributions of the individual inhibitors to these molecular alterations, we applied 3 nM quizartinib ± 400 nM adavosertib to MOLM-13 cells. Immunoblotting illustrated that quizartinib reduced WEE1, RRM2, and phosphorylated STAT5, and that adavosertib accentuated these effects in MOLM-13 cells (Fig. 5E, right panel). We detected a similar regulation of RRM2 by these drugs in MV4–11 cells (Fig. 5F).

DepMap analyses illustrate that leukemia cells rely on RRM2 which is consistent with its indispensable function for dNTP synthesis, S phase progression, and hence cell growth per se (Fig. 5G). Such a finding makes it tempting to speculate that higher levels of RRM2 in patients are linked to a more severe disease progression. RNA-sequencing data for 54 AML patients in the Gene Expression Profiling Interactive Analysis version 2 (GEPIA2) database show that high mRNA expression levels of *RRM2* correlate with a reduced overall survival of AML patients (Fig. 5H).

These data reveal that adavosertib and marbotinib deplete RRM2 which is an indispensable DNA replication protein and a possible prognostic marker.

3. Discussion

Treatment of AML patients with FLT3 mutants is unsatisfactory [2–4], necessitating the need for more preclinical and clinical investigations. Our results demonstrate that a combined application of quizartinib or marbotinib and adavosertib kills permanent and primary AML cells synergistically, without negative effects on normal human blood cells and murine hematopoietic progenitors. Thus, such drug combinations might be more effective at lower single drug concentrations and at the cost of less side effects in patients.

An advantage of quizartinib and adavosertib is that they have been evaluated in clinical trials and the corresponding safety and toxicology data in humans are publicly available, e.g., [5,35,48]. The FLT3 inhibitors gilteritinib and midostaurin are also approved for the treatment of AML that is associated with FLT3-ITD [1–4]. Thus, various clinically used FLT3 inhibitor plus adavosertib combinations are plausible with on the shelf medicines. Notably, authorities like the US Food-and-Drug-Administration no longer require animal tests before human drug trials [49]. Thus, combinations of inhibitors of hyperactive FLT3 and WEE1 may become a reality in foreseeable patient treatment settings.

As major mechanism underlying the observed synergistic, leukemia cell-specific cytotoxicity, we see a downregulation of the anti-apoptotic protein MCL1 and an accumulation of pro-apoptotic BIM. These BCL2 family proteins control mitochondrial integrity antagonistically. A shift in their balance towards pro-apoptotic BCL2 proteins disrupts mitochondrial membranes. These consequently release cytochrome c, which in complex with APAF1 activates the caspase-9 to caspase-3 cascade of apoptosis [39]. In line, recent data show that BIM is a key mediator of pro-apoptotic effects of FLT3 inhibitors in AML cells carrying FLT3-ITD [50]. The accumulation of BIM can be explained by the inactivation of AKT and ERK upon FLT3 inhibition. These phosphorylate BIM to

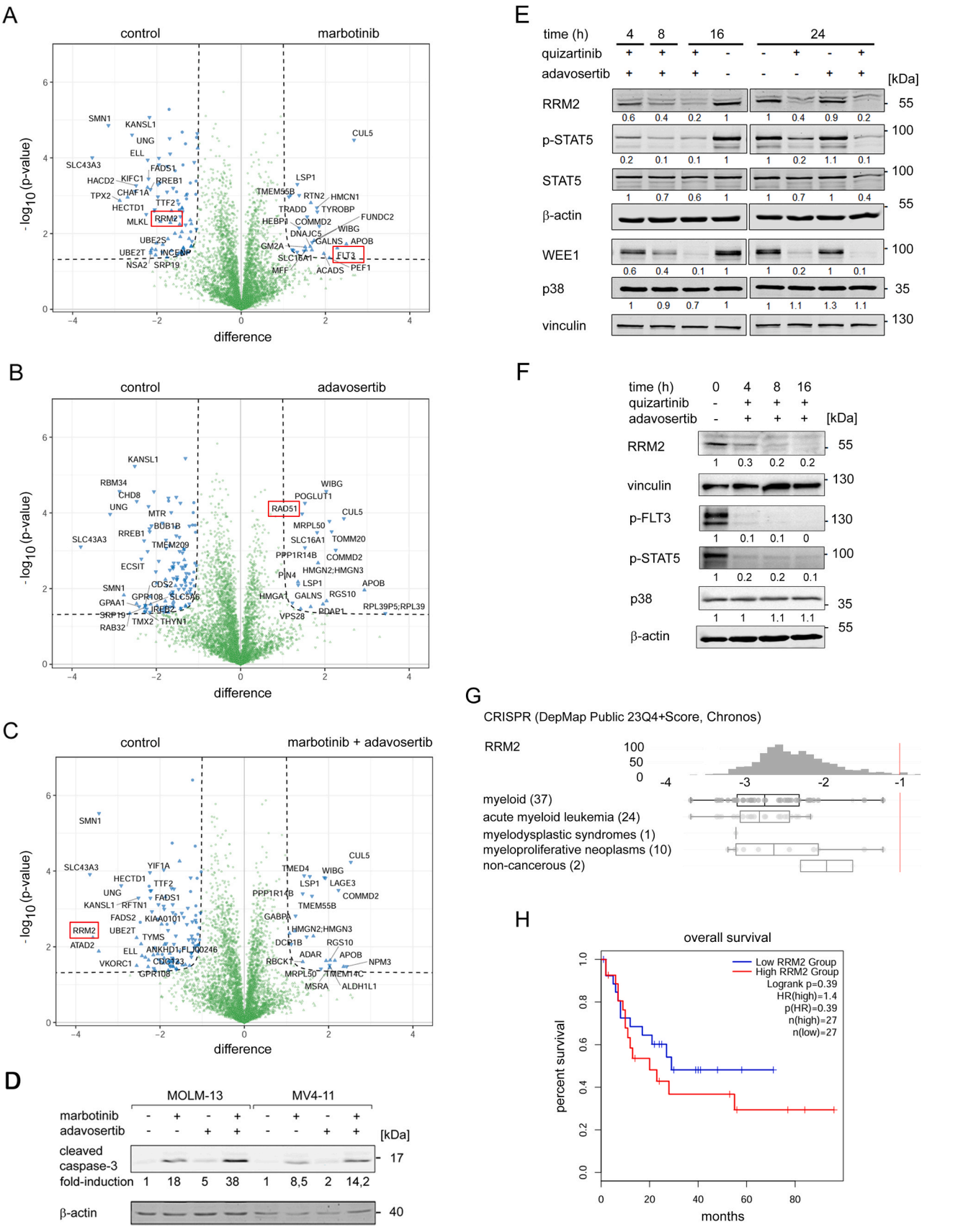

(caption on next page)

Fig. 5. Proteomic analysis and verification. MV4–11 cells were left untreated as controls or were incubated with A: marbotinib (3 nM), B: adavosertib (400 nM), or C: both for 24 h. Lysates were subjected to mass spectrometry in quadruplicates. Due to the sensitivity of proteomics, we used a water-soluble form of marbotinib for this assay [10]. D: Verification of apoptosis induction as accumulation of cleaved caspase-3 in leukemic cells that were incubated for 24 h with 3 nM marbotinib ± 400 nM adavosertib; β-actin, loading control; (n=2). E: MOLM-13 cells were treated with 3 nM quizartinib plus 400 nM adavosertib for 4, 8, and 16 h; the untreated control cell samples were collected at 16 h. Immunoblot analyses were conducted to assess how such treatment affected the indicated proteins (left). The right panel shows the levels of the same proteins in response to 3 nM quizartinib ± 400 nM adavosertib after 24 h. The numbers are intensities of the measured protein bands divided by the corresponding loading controls; (n=2). F: MV4–11 cells were treated with 3 nM quizartinib plus 400 nM adavosertib for 0–16 h. Immunoblots were done for the shown proteins; numbers are intensities of the measured protein bands divided by the corresponding loading controls; (n=2). The loss of the phosphorylated forms of FLT3 and STAT5 is a positive control for drug efficacy. G: DepMap project data show the dependency of all analyzed cell types (upper panel) and specifically of myeloid leukemia cells on FLT3 and WEE1; the dependency cutoff is −1 and indicated by a red line. Common essential genes have a dependency score of −1 and less (up to 100 % counterselection against cells with the knockdown, growth arrest or killing; https://forum.depmap.org/t/depmap-genetic-dependencies-faq/131; RRM2 DepMap Gene Summary). H: the GEPIA2 database shows that the overall survival of AML patients has a trend to inversely correlate with the expression of *RRM2* mRNA; (cancer-pku.cn).

promote its proteasomal degradation [51]. This is not contradicted by an increase in FLT3-ITD in marbotinib-treated MV4–11 cells that we noted in proteomics assays, because the activating phosphorylation of FLT3-ITD can be suppressed completely by marbotinib [9,12]. Our data on a cleavage of MCL1 are consistent with data that were collected in head and neck squamous cell carcinoma. In such cells, the inhibition of WEE1 with adavosertib caused the cleavage of MCL1 and of another anti-apoptotic protein, XIAP, by caspases [52]. Our results that show that both adavosertib and quizartinib promote the processing of MCL1 into smaller forms and that this is augmented when synergistically pro-apoptotic concentrations of adavosertib and quizartinib are applied together to leukemia cells. Unlike MCL1, BCL2 is hardly altered by these agents, indicating a selective downregulation of anti-apoptotic factors by such drugs.

Further studies will decipher which other pro-apoptotic and anti-apoptotic factors are controlled upon inhibition of WEE1 and mutant FLT3 [39,40]. Notably, the transcription factor p53, which is associated with the prognosis of AML patients [41,42] and its activating post-translational modifications [43] seem not to be required for the synergistic killing of such cells by quizartinib and adavosertib. The loss of p21 that we show here in response to quizartinib confirms our previous data which disclose that quizartinib and marbotinib reduce p21 and augment the levels of the related cell cycle inhibitor p27 [9]. Our results that quizartinib attenuated the activating phosphorylation and expression of p53 can explain the reduction of p21 by this drug. Independent of these details, quizartinib and adavosertib kill FLT3-ITD-positive AML cells without the requirement for detectable activation of p53.

In newly diagnosed and relapsed AML cell lines and patient blasts, pharmacological inhibition of CHK1 accentuates anti-proliferative effects of adavosertib [38,53]. Our data show that quizartinib and adavosertib decrease CHK1 in MV4–11 cells. A combined inactivation of FLT3-ITD and WEE1 boosts the downregulation of CHK1 by either drug. Consistent herewith, inhibition of mutant FLT3 and CHK1 with an orally bioavailable dual FLT3/CHK1 inhibitor kills leukemic cells that carry FLT3-ITD and FLT3-TKD mutants [54].

We noted that DNA replication stress and DNA damage preceded apoptosis in leukemic cells that were treated with quizartinib and adavosertib. Hence, the induction of such stress appears as molecular mechanisms through which inhibitors of FLT3 and WEE1 kill leukemic cells. The rapid downregulation of RRM2 can explain the early induction of DNA replication stress and DNA lesions, which precede apoptosis. It was published that the catalytic activity of WEE1 supported the expression and stability of RRM2 in solid tumor-derived cells [18,23]. Our unbiased mass spectrometry-based proteomics show that the inhibitory impact of FLT3 inhibition on RRM2 is stronger than that of WEE1 inhibition and that this effect is reproducible in independent human AML cell models with FLT3-ITD. This robust effect of quizartinib and marbotinib on RRM2 might be explained by the elimination of WEE1 , but likewise by yet undefined other pathways. Unlike FLT3 inhibitors, the ATP-competitive WEE1 inhibitor adavosertib targets WEE1 but not its upstream regulators or its total levels in such cells. From these data, we deduce further that hyperactive FLT3 strongly induces WEE1 gene expression and/or posttranslational modifications that stabilize WEE1. It is tempting to speculate that the hyperactivation of cell proliferation by FLT3-ITD requires WEE1 to sustain the cellular dNTP pools and to prevent excessive DNA replication origin firing that can result in lethal DNA replication stress. Cells with wild-type FLT3, including normal cells, have more controlled DNA replication. This may explain why they are less susceptible to inhibitors of FLT3 and WEE1.

The tetrameric ribonucleotide reductase complex RRM1/RRM2 catalyzes the *de novo* synthesis of dNTPs for DNA replication in S phase and for the repair of DNA lesions [24]. Thus, the depletion of RRM2 appears as a prominent factor in case of DNA replication stress/DNA damage induction upon inhibition of FLT3-ITD and WEE1. This is supported by time course analyses that show a temporal association between DNA replication stress/DNA damage and reduced RRM2 levels in leukemia cells. Furthermore, we previously showed that inhibitors of FLT3 and the RRM2 inhibitor hydroxyurea promoted their pro-apoptotic effects in such cells [55]. CHK1 is necessary for cell cycle control and to prevent the accumulation of DNA damage when RRM2 is inactivated genetically or with inhibitors [56,57]. Thus, the observed decrease in CHK1 expression upon treatment with inhibitors of FLT3 and WEE1 can likewise contribute to a failure of cells to arrest the cell cycle for DNA repair. The loss of RAD51 and HR can augment DNA injury under such circumstances. The regulation of both processes by adavosertib can explain why it promotes the pro-apoptotic effects of quizartinib and marbotinib in rapidly growing leukemia cells.

Taken together, we reveal a new, synergistically active drug combination that might become relevant for the treatment of patients suffering from hard-to-treat AML. The induction of DNA replication stress and DNA damage due to a loss of RRM2 appears to be a major molecular mechanism and marker for such beneficial drug interactions. Their primary endpoint is apoptosis of AML cells with mutant FLT3.

4. Material and methods

4.1. Drugs and chemicals

Triton X-100 and propidium iodide (PI) were purchased from Sigma-Aldrich Chemie GmbH, Munich, Germany; Z-VAD-FMK was from Selleck Chemicals, Munich, Germany; dithiothreitol was from PanReac AppliChem, Darmstadt, Germany; formalin (37 %) and bovine milk powder were from Carl Roth, Karlsruhe, Germany; the Fixable Viability Dye eFluor™ 780 was from Thermo Fisher, Frankfurt/Main, Germany.

4.2. Cell culture, PBMCs, primary AML patient cells with ethics declaration, and primary mouse cells

MV4–11 cells (DSMZ #ACC102) and MOLM-13 cells (DSMZ #ACC554) were cultured in RPMI-1640, supplemented with 10 % fetal calf serum (FCS, Lonza, Cologne, Germany) and 1 % penicillin/streptomycin (Sigma, Munich, Germany). Both cell cultures were kind gifts from Prof. Dr. F.-D. Böhmer, Jena University Medical Center, and originally from the DSMZ, Braunschweig, Germany. The cells were

authenticated by DNA fingerprint profiling using eight different and highly polymorphic short tandems repeats at the DSMZ, and regularly excluded to have mycoplasma by enzymatic tests. Experiments with PBMCs were done in accordance with ethic approval by the Landesärztekammer Rhineland-Palatine no.: 837.258.17 (11092). The PBMCs from healthy donors were isolated using Biocoll (Bio&Sell, Feucht, Germany) for gradient centrifugation and cultured in the above-mentioned growth medium. These cells were tested negative for common infections [58]. To identify cell populations, we used the antibodies CD11b BV510 (#101263), CD1c BV605 (#331538), CD3 BV711 (#344838) from BioLegend; CD14 PE-eFl610 (#61–0149–42), CD56 Pe-Cy7 (#25–0567–42), CD19 AF488 (#53–0199–42) from ThermoFisher. To determine their fitness, cells were stained with annexin-V AF647 (#A23204; early apoptosis marker) and FVD eFl780 (#65–0865–18; late apoptosis marker; both from ThermoFisher). Fresh primary AML peripheral blood samples were obtained from patients with *de novo* AML, following written informed consent and in accordance with the National Cancer Research Institute (NCRI) AML trial bank regulations and the Declaration of Helsinki under ethical approval REC: 17/LO/1566. Mononuclear cells were separated and cultured as described by us in [59]. For the primary murine bone marrow isolation and analysis, C57BL/6 mice were sacrificed, the tibiae, femurs and hip bones from the hind legs were removed and excess muscle tissue was removed. Bone marrow tissues were flushed out with medium using a syringe and the resulting bone marrow suspensions were filtered through 40 μM strainers. After lysis of erythrocytes, cells were counted, seeded into 12-well plates at a concentration of 10^6/mL, and treated with inhibitors. After 24 h, cells were harvested for flow cytometry analysis after staining with the antibodies SCA-1-FITC (clone: D7, eBioscience 11–5981–81), c-KIT-APC (clone: ACK2, Thermo Fisher Scientific 17–1172–82), CD3-PE (clone: 17A2, BioLegend 100206), CD4-PE (clone: RM4–5, eBioscience 12–0042–83), CD8-PE (clone: M18/2, BioLegend 101408), CD11b-PE (clone: M1/70, BD 553311), CD19-PE (clone: 1D3, PharMingen 557399), NK1.1-PE (clone: PK136, eBioscience 12–5941–83), Gr-1-PE (clone: RB6–8C5, eBioscience 12–5931–81) and Fixable Viability Dye eFluor® 780. The graphs were created with GraphPad Prism 6.0.

4.3. Protein detection

Immunoblot analyses were performed as described by us [60]. Membranes were blocked with 5 % milk powder diluted in TBS-tween-20. Antibodies were diluted in 2 % milk/TBS-tween-20. Antibodies were used at the indicated dilutions and were purchased from Cell Signaling, Frankfurt/Main, Germany: p-FLT3 (Tyr591) (cs-3461), 1:250; p-AKT (Ser473) (cs-9271S), 1:1000; p-CDK1 (Tyr15), (9111), 1:500; p-p38 (Thr180, Tyr182) (cs-9215), 1:100; CHK1 (cs-2360), 1:1000; p-ERK1/p-ERK2 (Thr202/Tyr204) (cs-9101), 1:1000; FLT3 (cs-3462), 1:500; cleaved caspase-3 (cs-9661); ERK1/ERK2 (p44/42) (cs-9102), 1:500; γH2AX (Ser139) (cs-9718), 1:1000; HSP90 (cs-4877), 1:1000; WEE1 (cs-4936), 1:500; p-p53 S15 (cs-9284), 1:500; ac-p53 K382 (cs-2525), 1:500; Novus Biologicals, Wiesbaden, Germany: β-actin (sc-47778), 1:5000; Abcam, Cambridge, UK: BAK (ab32371), 1:500; BIM (ab32158), 1:1000; AKT (abcam-32505), 1:500; p38 (ab31828), 1:1000; RAD51 (ab6380), 1:1000; p21 (ab109520), 1:1000; Thermo Fisher, Frankfurt/Main: RRM2 (PA5–13570), 1:500; p-STAT5 (Tyr694) (#MA5–14973), 1:500; BD Biosciences, Franklin Lakes, USA (610191), 1:1000; Santa Cruz, Heidelberg, Germany: anti-β-actin (sc-47778), 1:1000; MCL-1 (sc-819), 1:1000; BCL2 (sc-7382), 1:500; p53 (sc-71817) 1:1000. Membranes were incubated with LI-COR infrared fluorescence secondary antibodies (1:10,000). Proteins were detected using Odyssey Infrared Imaging System (LICOR). Data analyses were done by Image Studio Lite V4.0 (LICOR).

4.4. Measurement of cell viability by flow cytometry

Cells were collected in FACS tubes and centrifuged (300 g for 5 min) at 4°C. The supernatants were discarded, pellets were resuspended in PBS, and centrifuged at 300 g at 4°C for 5 min. For live/dead measurement, cells were resuspended in 200 μL PBS and 4′,6-Diamidin-2-phenylindol (DAPI) was added to the cells at 3.6 μM right before measurement. For a more detailed lived/dead staining, the cells were incubated with the mitochondrial integrity dye 3,3′-dihexyloxacarbocyaniniodid (DIOC6) at 50 nM for 30 min right before harvesting and were subsequently stained with DAPI. PBMCs were stained with the Fixable Viability Dye eFluor® 780 for live/dead analysis. DAPI cannot sufficiently penetrate intact cell membranes and is therefore not taken up by living cells. Due to cell death, the cell membrane becomes porous and DAPI can bind to DNA which increases its emission 20-fold. DIOC6 binds specifically to mitochondria and therefore accumulates in living cells. DIOC6-positive cells are alive, with intact mitochondria. DIOC6-negative/DAPI-negative cells are early apoptotic, with a decrease of DIOC6 due mitochondrial injury. DIOC6-negative/DAPI-positive cells are late apoptotic, with disrupted mitochondria and lost plasma membrane integrity. The cells were measured with a FACS Canto II flow cytometer and analyzed with the BD FACSDiva™ Software (BD Biosciences, Heidelberg, Germany). Analysis of apoptosis by annexin-V-FITC/propidium iodine (PI) staining: MV4–11 cells were harvested, stained with annexin-V-FITC and propidium iodide (PI), and analyzed for apoptosis as previously described [60].

4.5. Cell cycle analysis by flow cytometry

Cells were collected in FACS tubes and centrifuged at 300 g at 4°C for 5 min and washed once with PBS. Afterwards, cells were resuspended in 200 μL hypotonic HFS buffer containing 3.88 mM sodium citrate and 0.1 % (v/v) Triton X-100. This led to permeabilization of the cells. Next, 2 μL of 50 μg/mL PI were added, and cells were measured with a FACS Canto II flow cytometer. Since PI binds to DNA, the signal correlated to DNA content in the cells which is 2 n during G1 phase and 4 n in G2 phase. During replication (S phase), the DNA content is between 2 n and 4 n.

4.6. MTT assay

This method was described in reference [61].

4.7. Immunofluorescence analyses

MV4–11 cells were treated with the inhibitors, harvested, resuspended in 20 μL PBS and pipetted onto coverslips. After drying, the cells were fixed in an acetone-methanol-solution (3:7) at −20 °C for 9 min and washed once with PBS. Blocking solution (10 % BSA, 0.25 % Triton X-100 in PBS) was added and incubated for 1 h at room temperature. Incubation with the primary antibodies, diluted in blocking solution, was carried out overnight in a wet chamber at 4 °C. Antibodies against RPA (1:500) and 53BP1 (1:500) and γH2AX (1:500) were used. The next day, the coverslips were washed thrice with PBS and incubated for 1 h at room temperature with secondary antibodies (1:300, diluted in blocking solution). Secondary antibodies coupled to AlexaFluor-488 (green) for immunofluorescence were from Thermo Fisher (Frankfurt/Main, Germany) and fluorescent secondary antibodies coupled to Cy3 (red) were from Jackson Immuno Research (Cambridgeshire, UK). Cells were washed twice with PBS, once with high salt PBS (0.4 M NaCl in PBS) for 2 min, and once more with PBS. Using a scalpel and tweezers, we carefully placed the coverslips on a slide and added 10 μL Vectashield® (Biozol, Vec-H-1.000) containing TO-PRO™-3 (Thermo Fisher, T3605) in a dilution of 1:100 to stain the nuclei. Images were captured with the confocal microscopy Zeiss Axio Observer.Z1 microscope equipped with an LSM710 laser-scanning unit (Carl Zeiss, Jena, Germany). Analysis

was performed with ImageJ software.

4.8. DepMap and GEPIA2 database analyses

The DepMap project is a collaborative effort of Broad Institute and Wellcome Sanger Institute. The analyzed proteins were eliminated by CRISPR-Cas9, and 14 days later pooled cells were examined for sgRNA expression. Negative values indicate dependency, 0 means no impact (https://forum.depmap.org/t/depmap-genetic-dependencies-faq/131). The GEPIA2 resource for gene expression data relies on cancer cell gene expression data within the RNA-sequencing-based databases TCGA and GTEx [62].

4.9. Proteomics

MV4–11 cells were left untreated as controls or were incubated with marbotinib (3 nM), adavosertib (400 nM), or both for 24 h. The experiment was conducted in quadruplicate and due to the sensitivity of proteomics, we used a water-soluble form of marbotinib for this assay [10]. The cells were lysed in 1x LDS buffer (Thermo Fisher) and run on a precast 4–12 % NuPage NOVEX PAGE gel (Thermo Fisher) at 180 V for 10 min. In gel digest was performed by mincing the gel pieces, reduction with DTT (Sigma-Aldrich), alkylation with IAA (Sigma-Aldrich) and subsequent digest with MS-grade trypsin (Serva, Heidelberg, Germany). The tryptic peptides were desalted and stored on a StageTip [63]. The peptides were fractionated on Easy-nLC 1200 (Thermo Fisher) by reverse-phase separation on a nanocapillary column packed with C18 material (Dr. Maisch GmbH, Ammerbuch, Germany) during a 2 h gradient from 4 % to 35 % ACN (VWR) and measured using data-dependent acquisition on an Exploris 480 mass spectrometer (Thermo Fisher). Data was analyzed with MaxQuant version 1.6.5.0 [64] using a human Uniprot protein database (81,194 entries) and standard settings except activated LFQ quantification on unique peptides. The data was filtered for contaminants, reverse hits and proteins only identified by site. Missing values were imputed, and the data plotted as a volcano plot with the median enrichment value versus the p-value (Welsh t-test).

4.10. Synergy calculation and statistics

Synergy was determined using the Combenefit free software [36]. The drug interaction models highest single agent (HSA), Loewe, and Bliss were used to determine synergism scores. Scores are interpreted as antagonistic effects: $x \leq -10$; no interaction effects: $-10 \leq x \leq 10$; synergistic effects: $x \geq 10$.

Statistical analyses were conducted using one-way or two-way ANOVA and unpaired t-test from GraphPad Prism 6 software. Correction of statistical analyses was achieved with Bonferroni multiple comparison; *p* values indicate statistical significances as indicated in the Figure legends.

Funding

Work done in the group of OHK is funded by the German Research Foundation/Deutsche Forschungsgemeinschaft (DFG) KR2291/12–1, project number 445785155; DFG KR2291/14–1, project number 469954457; KR2291/15–1, project number 495271833; KR2291/16–1, project number 496927074; KR2291/17–1, project number 502534123; KR2291/18–1, project number 528202295; funded by the Deutsche Forschungsgemeinschaft (DFG, German Research Foundation) – Project-ID 393547839 – SFB 1361; the DAAD Egypt/Germany; the Brigitte und Dr. Konstanze Wegener-Stiftung (projects 65/110); and the Walter Schulz-Stiftung.

CRediT authorship contribution statement

Walburgis Brenner: Resources. **Matthias Bros:** Resources, Formal analysis. **Falk Butter:** Formal analysis, Resources. **Al-Hassan M. Mustafa:** Writing – original draft, Methodology, Investigation, Formal analysis. **Oliver H. Krämer:** Writing – review & editing, Writing – original draft, Visualization, Supervision, Project administration, Funding acquisition, Formal analysis, Conceptualization. **Christoph Hieber:** Validation, Methodology, Investigation. **Hans-Peter Wollscheid:** Writing – original draft, Conceptualization. **Sven Henninger:** Formal analysis, Conceptualization. **Michelle Lazenby:** Methodology, Investigation. **Sarah Neuroth:** Investigation, Validation. **Joanna Zabkiewicz:** Methodology, Formal analysis, Conceptualization. **Siavosh Mahboobi:** Resources. **Caroline Alvares:** Resources.

Declaration of Competing Interest

OHK declares paid consultant activity for BASF, Ludwigshafen, Germany, and the patent "The use of molecular markers for the preclinical and clinical profiling of inhibitors of enzymes having histone deacetylase activity". The BASF has not influenced our study and its products are not discussed in the manuscript. SM and OHK declare the patents "Novel HDAC6 inhibitors and their uses", and "Synthesis, pharmacology and use of new and selective FMS-like tyrosine kinase 3 (FLT3) inhibitors". All other authors declare that they have no conflict of interest.

Data Availability

The mass spectrometry-based proteomics data have been deposited to the ProteomeXchange Consortium via the PRIDE partner repository with the dataset identifier PXD051340.

Acknowledgement

We thank Andrea Piée-Staffa and Christina Brachetti, Mainz University Medical Center, for excellent technical support. Prof. Dr. Oliver Ottmann, University of Cardiff, UK was an invaluable discussion partner throughout the project. We thank Prof. Dr. F.-D. Böhmer, Institute of Molecular Cell Biology, CMB, Jena University Hospital, Jena, Germany, for leukemic cell lines. We thank the Blood transfusion unit of the University Medical Center Mainz for providing us with buffy coats for PBMC isolation.

Appendix A. Supporting information

Supplementary data associated with this article can be found in the online version at doi:10.1016/j.biopha.2024.117076.

References

[1] J.U. Kazi, L. Ronnstrand, FMS-like tyrosine Kinase 3/FLT3: from basic science to clinical implications, Physiol. Rev. 99 (3) (2019) 1433–1466.
[2] N. Daver, R.F. Schlenk, N.H. Russell, M.J. Levis, Targeting FLT3 mutations in AML: review of current knowledge and evidence, Leukemia 33 (2) (2019) 299–312.
[3] A.E. Perl, Availability of FLT3 inhibitors: how do we use them? Blood 134 (9) (2019) 741–745.
[4] A.I. Antar, Z.K. Otrock, E. Jabbour, M. Mohty, A. Bazarbachi, FLT3 inhibitors in acute myeloid leukemia: ten frequently asked questions, Leukemia 34 (3) (2020) 682–696.
[5] H.P. Erba, P. Montesinos, H.J. Kim, E. Patkowska, R. Vrhovac, P. Zak, P.N. Wang, T. Mitov, J. Hanyok, Y.M. Kamel, J.E.C. Rohrbach, L. Liu, A. Benzohra, A. Lesegretain, J. Cortes, A.E. Perl, M.A. Sekeres, H. Dombret, S. Amadori, J. Wang, M.J. Levis, R.F. Schlenk, A.-F.S.G. Qu, Quizartinib plus chemotherapy in newly diagnosed patients with FLT3-internal-tandem-duplication-positive acute myeloid leukaemia (QuANTUM-First): a randomised, double-blind, placebo-controlled, phase 3 trial, Lancet 401 (10388) (2023) 1571–1583.
[6] C.C. Smith, Q. Wang, C.S. Chin, S. Salerno, L.E. Damon, M.J. Levis, A.E. Perl, K. J. Travers, S. Wang, J.P. Hunt, P.P. Zarrinkar, E.E. Schadt, A. Kasarskis, J. Kuriyan,

N.P. Shah, Validation of ITD mutations in FLT3 as a therapeutic target in human acute myeloid leukaemia, Nature 485 (7397) (2012) 260–263.
[7] C.C. Smith, E.A. Lasater, K.C. Lin, Q. Wang, M.Q. McCreery, W.K. Stewart, L. E. Damon, A.E. Perl, G.R. Jeschke, M. Sugita, M. Carroll, S.C. Kogan, J. Kuriyan, N. P. Shah, Crenolanib is a selective type I pan-FLT3 inhibitor, Proc. Natl. Acad. Sci. USA 111 (14) (2014) 5319–5324.
[8] A. Galanis, H. Ma, T. Rajkhowa, A. Ramachandran, D. Small, J. Cortes, M. Levis, Crenolanib is a potent inhibitor of FLT3 with activity against resistance-conferring point mutants, Blood 123 (1) (2014) 94–100.
[9] M. Beyer, S.J. Henninger, P.S. Haehnel, A.M. Mustafa, E. Gurdal, B. Schubert, M. Christmann, A. Sellmer, S. Mahboobi, S. Drube, W. Sippl, T. Kindler, O. H. Krämer, Identification of a highly efficient dual type I/II FMS-like tyrosine kinase inhibitor that disrupts the growth of leukemic cells, Cell Chem. Biol. 29 (3) (2022) 398–411, e394.
[10] S. Opatz, H. Polzer, T. Herold, N.P. Konstandin, B. Ksienzyk, E. Zellmeier, S. Vosberg, A. Graf, S. Krebs, H. Blum, K.P. Hopfner, P.M. Kakadia, S. Schneider, A. Dufour, J. Braess, M.C. Sauerland, W.E. Berdel, T. Buchner, B.J. Woermann, W. Hiddemann, K. Spiekermann, S.K. Bohlander, P.A. Greif, Exome sequencing identifies recurring FLT3 N676K mutations in core-binding factor leukemia, Blood 122 (10) (2013) 1761–1769.
[11] K. Huang, M. Yang, Z. Pan, F.H. Heidel, M. Scherr, M. Eder, T. Fischer, G. Busche, K. Welte, N. von Neuhoff, A. Ganser, Z. Li, Leukemogenic potency of the novel FLT3-N676K mutant, Ann. Hematol. 95 (5) (2016) 783–791.
[12] A. Sellmer, B. Pilsl, M. Beyer, H. Pongratz, L. Wirth, S. Elz, S. Dove, S.J. Henninger, K. Spiekermann, H. Polzer, S. Klaeger, B. Küster, F.D. Böhmer, H.H. Fiebig, O. H. Krämer, S. Mahboobi, A series of novel aryl-methanone derivatives as inhibitors of FMS-like tyrosine kinase 3 (FLT3) in FLT3-ITD-positive acute myeloid leukemia, Eur. J. Med Chem. 193 (2020) 112232.
[13] A. Ghelli Luserna di Rora, C. Cerchione, G. Martinelli, G. Simonetti, A WEE1 family business: regulation of mitosis, cancer progression, and therapeutic target, J. Hematol. Oncol. 13 (1) (2020) 126.
[14] C.J. Matheson, D.S. Backos, P. Reigan, Targeting WEE1 kinase in cancer, Trends Pharm. Sci. 37 (10) (2016) 872–881.
[15] A. Abou Zahr, G. Borthakur, Emerging cell cycle inhibitors for acute myeloid leukemia, Expert Opin. Emerg. Drugs 22 (2) (2017) 137–148.
[16] K. Mahajan, N.P. Mahajan, WEE1 tyrosine kinase, a novel epigenetic modifier, Trends Genet 29 (7) (2013) 394–402.
[17] C.R. Elbaek, V. Petrosius, J. Benada, L. Erichsen, R.B. Damgaard, C.S. Sørensen, WEE1 kinase protects the stability of stalled DNA replication forks by limiting CDK2 activity, Cell Rep. 38 (3) (2022) 110261.
[18] H. Beck, V. Nahse-Kumpf, M.S. Larsen, K.A. O'Hanlon, S. Patzke, C. Holmberg, J. Mejlvang, A. Groth, O. Nielsen, R.G. Syljuasen, C.S. Sorensen, Cyclin-dependent kinase suppression by WEE1 kinase protects the genome through control of replication initiation and nucleotide consumption, Mol. Cell Biol. 32 (20) (2012) 4226–4236.
[19] R. Domínguez-Kelly, Y. Martin, S. Koundrioukoff, M.E. Tanenbaum, V.A. Smits, R. H. Medema, M. Debatisse, R. Freire, Wee1 controls genomic stability during replication by regulating the Mus81-Eme1 endonuclease, J. Cell Biol. 194 (4) (2011) 567–579.
[20] H. Duda, M. Arter, J. Gloggnitzer, F. Teloni, P. Wild, M.G. Blanco, M. Altmeyer, J. Matos, A mechanism for controlled breakage of under-replicated chromosomes during mitosis, Dev. Cell 39 (6) (2016) 740–755.
[21] K. Mahajan, B. Fang, J.M. Koomen, N.P. Mahajan, H2B Tyr37 phosphorylation suppresses expression of replication-dependent core histone genes, Nat. Struct. Mol. Biol. 19 (9) (2012) 930–937.
[22] T.B. Garcia, J.C. Snedeker, D. Baturin, L. Gardner, S.P. Fosmire, C. Zhou, C. T. Jordan, S. Venkataraman, R. Vibhakar, C.C. Porter, A Small-Molecule Inhibitor of WEE1, AZD1775, synergizes with olaparib by impairing homologous recombination and enhancing DNA damage and apoptosis in acute Leukemia, Mol. Cancer Ther. 16 (10) (2017) 2058–2068.
[23] S.X. Pfister, E. Markkanen, Y. Jiang, S. Sarkar, M. Woodcock, G. Orlando, I. Mavrommati, C.C. Pai, L.P. Zalmas, N. Drobnitzky, G.L. Dianov, C. Verrill, V. M. Macaulay, S. Ying, N.B. La Thangue, V. D'Angiolella, A.J. Ryan, T.C. Humphrey, Inhibiting WEE1 selectively kills histone H3K36me3-deficient cancers by dNTP starvation, Cancer Cell 28 (5) (2015) 557–568.
[24] Y. Zhan, L. Jiang, X. Jin, S. Ying, Z. Wu, L. Wang, W. Yu, J. Tong, L. Zhang, Y. Lou, Y. Qiu, Inhibiting RRM2 to enhance the anticancer activity of chemotherapy, Biomed. Pharm. 133 (2021) 110996.
[25] F. Neizer-Ashun, R. Bhattacharya, Reality CHEK: understanding the biology and clinical potential of CHK1, Cancer Lett. 497 (2021) 202–211.
[26] H. Goto, T. Natsume, M.T. Kanemaki, A. Kaito, S. Wang, E.C. Gabazza, M. Inagaki, A. Mizoguchi, Chk1-mediated Cdc25A degradation as a critical mechanism for normal cell cycle progression, J. Cell Sci. 132 (2) (2019).
[27] K. Neben, S. Schnittger, B. Brors, B. Tews, F. Kokocinski, T. Haferlach, J. Muller, M. Hahn, W. Hiddemann, R. Eils, P. Lichter, C. Schoch, Distinct gene expression patterns associated with FLT3- and NRAS-activating mutations in acute myeloid leukemia with normal karyotype, Oncogene 24 (9) (2005) 1580–1588.
[28] Y. Zhang, L. Yuan, Fms-like tyrosine kinase 3-internal tandem duplications epigenetically activates checkpoint kinase 1 in acute myeloid leukemia cells, Sci. Rep. 11 (1) (2021) 13236.
[29] V. Wachholz, A.M. Mustafa, Y. Zeyn, S.J. Henninger, M. Beyer, M. Dzulko, A. Piee-Staffa, C. Brachetti, P.S. Haehnel, A. Sellmer, S. Mahboobi, T. Kindler, W. Brenner, T. Nikolova, O.H. Krämer, Inhibitors of class I HDACs and of FLT3 combine synergistically against leukemia cells with mutant FLT3, Arch. Toxicol. 96 (1) (2022) 177–193.
[30] K.A. Cole, S. Pal, R.A. Kudgus, H. Ijaz, X. Liu, C.G. Minard, B.R. Pawel, J.M. Maris, D.A. Haas-Kogan, S.D. Voss, S.L. Berg, J.M. Reid, E. Fox, B.J. Weigel, Phase I clinical trial of the Wee1 inhibitor adavosertib (AZD1775) with irinotecan in children with relapsed solid tumors. A COG Phase I consortium report (ADVL1312), Clin. Cancer Res (2019).
[31] K.C. Cuneo, M.A. Morgan, V. Sahai, M.J. Schipper, L.A. Parsels, J.D. Parsels, T. Devasia, M. Al-Hawaray, C.S. Cho, H. Nathan, J. Maybaum, M.M. Zalupski, T. S. Lawrence, Dose escalation trial of the Wee1 Inhibitor Adavosertib (AZD1775) in combination with gemcitabine and radiation for patients with locally advanced pancreatic cancer, J. Clin. Oncol. 37 (29) (2019) 2643–2650.
[32] J.F. Liu, N. Xiong, S.M. Campos, A.A. Wright, C. Krasner, S. Schumer, N. Horowitz, J. Veneris, N. Tayob, S. Morrissey, G. West, R. Quinn, U.A. Matulonis, P. A. Konstantinopoulos, Phase II study of the WEE1 inhibitor adavosertib in recurrent uterine serous carcinoma, J. Clin. Oncol. 39 (14) (2021) 1531–1539.
[33] J. Liu, A.M. Oza, N. Colombo, A. Oaknin, ADAGIO: a phase IIb international study of the Wee1 inhibitor adavosertib in women with recurrent or persistent uterine serous carcinoma, Int J. Gynecol. Cancer 32 (1) (2022) 89–92.
[34] D. Shafer, A.B. Kagan, M.A. Rudek, M. Kmieciak, M.B. Tombes, E. Shrader, D. Bandyopadhyay, D. Hudson, H. Sankala, C. Weir, J.E. Lancet, S. Grant, Phase 1 study of belinostat and adavosertib in patients with relapsed or refractory myeloid malignancies, Cancer Chemother. Pharm. 91 (3) (2023) 281–290.
[35] G. Massacci, V. Venafra, S. Latini, V. Bica, G.M. Pugliese, S. Graziosi, F. Klingelhuber, N. Krahmer, T. Fischer, D. Mougiakakos, M. Boettcher, L. Perfetto, F. Sacco, A key role of the WEE1-CDK1 axis in mediating TKI-therapy resistance in FLT3-ITD positive acute myeloid leukemia patients, Leukemia 37 (2) (2023) 288–297.
[36] G.Y. Di Veroli, C. Fornari, D. Wang, S. Mollard, J.L. Bramhall, F.M. Richards, D. I. Jodrell, Combenefit: an interactive platform for the analysis and visualization of drug combinations, Bioinformatics 32 (18) (2016) 2866–2868.
[37] N. Dayal, C. Opoku-Temeng, D.E. Hernandez, M.A. Sooreshjani, B.A. Carter-Cooper, R.G. Lapidus, H.O. Sintim, Dual FLT3/TOPK inhibitor with activity against FLT3-ITD secondary mutations potently inhibits acute myeloid leukemia cell lines, Future Med Chem. 10 (7) (2018) 823–835.
[38] W. Qi, C. Xie, C. Li, J.T. Caldwell, H. Edwards, J.W. Taub, Y. Wang, H. Lin, Y. Ge, CHK1 plays a critical role in the anti-leukemic activity of the wee1 inhibitor MK-1775 in acute myeloid leukemia cells, J. Hematol. Oncol. 7 (2014) 53.
[39] F.J. Bock, S.W.G. Tait, Mitochondria as multifaceted regulators of cell death, Nat. Rev. Mol. Cell Biol. 21 (2) (2020) 85–100.
[40] S. Milnerowicz, J. Maszewska, P. Skowera, M. Stelmach, M. Lejman, AML under the Scope: Current Strategies and Treatment Involving FLT3 Inhibitors and Venetoclax-Based Regimens, Int J. Mol. Sci. 24 (21) (2023).
[41] D.Y. Shin, TP53 mutation in acute myeloid leukemia: an old foe revisited, Cancers (Basel) 15 (19) (2023).
[42] J.E. Zawacka, p53 biology and reactivation for improved therapy in MDS and AML, Biomark. Res 12 (1) (2024) 34.
[43] J. Wen, D. Wang, Deciphering the PTM codes of the tumor suppressor p53, J. Mol. Cell Biol. 13 (11) (2022) 774–785.
[44] L.I. Toledo, M. Altmeyer, M.B. Rask, C. Lukas, D.H. Larsen, L.K. Povlsen, S. Bekker-Jensen, N. Mailand, J. Bartek, J. Lukas, ATR prohibits replication catastrophe by preventing global exhaustion of RPA, Cell 155 (5) (2013) 1088–1103.
[45] E.P. Rogakou, W. Nieves-Neira, C. Boon, Y. Pommier, W.M. Bonner, Initiation of DNA fragmentation during apoptosis induces phosphorylation of H2AX histone at serine 139, J. Biol. Chem. 275 (13) (2000) 9390–9395.
[46] J.E. Cleaver, . gammaH2Ax: biomarker of damage or functional participant in DNA repair "all that glitters is not gold!, Photochem. Photobio. 87 (6) (2011) 1230–1239.
[47] T. Nikolova, N. Kiweler, O.H. Krämer, Interstrand crosslink repair as a target for HDAC inhibition, Trends Pharm. Sci. 38 (9) (2017) 822–836.
[48] N.J. Short, D. Nguyen, F. Ravandi, Treatment of older adults with FLT3-mutated AML: emerging paradigms and the role of frontline FLT3 inhibitors, Blood Cancer J. 13 (1) (2023) 142.
[49] M. Wadman, FDA no longer has to require animal testing for new drugs, Science 379 (6628) (2023) 127–128.
[50] R. Zhu, L. Li, B. Nguyen, J. Seo, M. Wu, T. Seale, M. Levis, A. Duffield, Y. Hu, D. Small, FLT3 tyrosine kinase inhibitors synergize with BCL-2 inhibition to eliminate FLT3/ITD acute leukemia cells through BIM activation, Signal Transduct. Target Ther. 6 (1) (2021) 186.
[51] M.M. Rose, V.L. Espinoza, K.J. Hoff, L.A. Pike, V. Sharma, M.C. Hofmann, A.C. Tan, N. Pozdeyev, R.E. Schweppe, BCL2L11 Induction Mediates Sensitivity to Src and MEK1/2 inhibition in thyroid cancer, Cancers (Basel) 15 (2) (2023).
[52] N. Tanaka, A.A. Patel, J. Wang, M.J. Frederick, N.N. Kalu, M. Zhao, A.L. Fitzgerald, T.X. Xie, N.L. Silver, C. Caulin, G. Zhou, H.D. Skinner, F.M. Johnson, J.N. Myers, A. A. Osman, Wee-1 Kinase Inhibition Sensitizes High-Risk HPV+ HNSCC to apoptosis accompanied by downregulation of MCl-1 and XIAP Antiapoptotic Proteins, Clin. Cancer Res 21 (21) (2015) 4831–4844.
[53] L. Zhou, Y. Zhang, S. Chen, M. Kmieciak, Y. Leng, H. Lin, K.A. Rizzo, C.I. Dumur, A. Ferreira-Gonzalez, Y. Dai, S. Grant, A regimen combining the Wee1 inhibitor AZD1775 with HDAC inhibitors targets human acute myeloid leukemia cells harboring various genetic mutations, Leukemia 29 (4) (2015) 807–818.
[54] K. Jiang, X. Li, C. Wang, X. Hu, P. Wang, L. Tong, Y. Tu, B. Chen, T. Jin, T. Wang, H. Wang, Y. Han, R. Gui, J. Yang, T. Liu, J. Li, Y. Zhou, Dual inhibition of CHK1/FLT3 enhances cytotoxicity and overcomes adaptive and acquired resistance in FLT3-ITD acute myeloid leukemia, Leukemia 37 (3) (2023) 539–549.
[55] M. Pons, Y. Zeyn, S. Zahn, N. Mahendrarajah, B.D.G. Page, P.T. Gunning, R. Moriggl, W. Brenner, F. Butter, O.H. Krämer, Oncogenic kinase cascades induce

molecular mechanisms that protect leukemic cell models from lethal effects of De Novo dNTP synthesis inhibition, Cancers (Basel) 13 (14) (2021).
[56] L. Taricani, F. Shanahan, M.C. Malinao, M. Beaumont, D. Parry, A functional approach reveals a genetic and physical interaction between ribonucleotide reductase and CHK1 in mammalian cells, PLoS One 9 (11) (2014) e111714.
[57] A. Göder, C. Emmerich, T. Nikolova, N. Kiweler, M. Schreiber, T. Kühl, D. Imhof, M. Christmann, T. Heinzel, G. Schneider, O.H. Krämer, HDAC1 and HDAC2 integrate checkpoint kinase phosphorylation and cell fate through the phosphatase-2A subunit PR130, Nat. Commun. 9 (1) (2018) 764.
[58] Y. Zeyn, K. Hausmann, M. Halilovic, M. Beyer, H.S. Ibrahim, W. Brenner, S. Mahboobi, M. Bros, W. Sippl, O.H. Krämer, Histone deacetylase inhibitors modulate hormesis in leukemic cells with mutant FMS-like tyrosine kinase-3, Leukemia 37 (11) (2023) 2319–2323.
[59] J. Zabkiewicz, M. Lazenby, G. Edwards, C.A. Bygrave, N. Omidvar, L. Zhuang, S. Knapper, C. Guy, R.K. Hills, A.K. Burnett, C.L. Alvares, Combination of a mitogen-activated protein kinase inhibitor with the tyrosine kinase inhibitor pacritinib combats cell adhesion-based residual disease and prevents re-expansion of FLT3-ITD acute myeloid leukaemia, Br. J. Haematol. 191 (2) (2020) 231–242.
[60] M.A. Fischer, A.M. Mustafa, K. Hausmann, R. Ashry, A.G. Kansy, M.C. Liebl, C. Brachetti, A. Piée-Staffa, M. Zessin, H.S. Ibrahim, T.G. Hofmann, M. Schutkowski, W. Sippl, O.H. Krämer, Novel hydroxamic acid derivative induces apoptosis and constrains autophagy in leukemic cells, J. Adv. Res S2090-1232 (23) (2023), 00197-00192.
[61] O.H. Krämer, D. Baus, S.K. Knauer, S. Stein, E. Jäger, R.H. Stauber, M. Grez, E. Pfitzner, T. Heinzel, Acetylation of Stat1 modulates NF-kappaB activity. Genes Dev. 20 (4) (2006) 473–485.
[62] J. Tang, P. Gautam, A. Gupta, L. He, S. Timonen, Y. Akimov, W. Wang, A. Szwajda, A. Jaiswal, D. Turei, B. Yadav, M. Kankainen, J. Saarela, J. Saez-Rodriguez, K. Wennerberg, T. Aittokallio, Network pharmacology modeling identifies synergistic Aurora B and ZAK interaction in triple-negative breast cancer, NPJ Syst. Biol. Appl. 5 (2019) 20.
[63] J. Rappsilber, M. Mann, Y. Ishihama, Protocol for micro-purification, enrichment, pre-fractionation and storage of peptides for proteomics using StageTips, Nat. Protoc. 2 (8) (2007) 1896–1906.
[64] J. Cox, M. Mann, MaxQuant enables high peptide identification rates, individualized p.p.b.-range mass accuracies and proteome-wide protein quantification, Nat. Biotechnol. 26 (12) (2008) 1367–1372.